Earth Syst. Sci. Data Discuss., 5, 1035–1056, 2012
www.earth-syst-sci-data-discuss.net/5/1035/2012/
doi:10.5194/essdd-5-1035-2012

Earth System Science Data Discussions
Open Access

Unmanned aircraft system measurements of the atmospheric boundary layer over Terra Nova Bay, Antarctica

S. L. Knuth[1], J. J. Cassano[1], J. A. Maslanik[2], P. D. Herrmann[3], P. A. Kernebone[3], R. I. Crocker[2], and N. J. Logan[3]

[1]Cooperative Institute for Research in Environmental Studies and Department of Atmospheric and Oceanic Sciences, University of Colorado, Boulder, Colorado, USA
[2]Department of Aerospace Engineering Sciences, University of Colorado, Boulder, Colorado, USA
[3]Aerosonde Pty Ltd, Melbourne, Australia

Received: 19 October 2012 – Accepted: 2 November 2012 – Published: 13 November 2012

Correspondence to: J. J. Cassano (john.cassano@colorado.edu)

Published by Copernicus Publications.

Abstract

In September 2009, a series of long-range unmanned aircraft system (UAS) flights collected basic atmospheric data over the Terra Nova Bay polynya in Antarctica. Air temperature, wind, pressure, relative humidity, radiation, skin temperature, GPS, and operational aircraft data were collected and quality controlled for scientific use. The data has been submitted to the United States Antarctic Program Data Coordination Center (USAP-DCC) for free access (doi:10.1594/USAP/0739464).

1 Introduction

Within the Terra Nova Bay (TNB) region of Antarctica, strong air-sea interactions occur during the winter months due to the presence of a persistent latent heat polynya generated largely due to strong downslope winds originating from the interior of the continent (Kurtz and Bromwich, 1983; Ciappa et al., 2012). These air-sea interactions are strongest during the winter months as the downslope and katabatic winds bring cold, dry air in contact with the relatively warmer and moister air overlying the polynya. Understanding the impacts of these two interacting air masses on atmospheric storms, energy transfer to and from the atmosphere, and the changing properties of oceanic water are important for furthering our knowledge of both local and large-scale meteorological, glaciological, and oceanographic changes. In September 2009, a series of unmanned aircraft system (UAS) flights were undertaken over the TNB polynya to measure changes in the atmospheric layer overlying the polynya (Cassano et al., 2010). The UAS used were built and designed by Aerosonde®, and collected atmospheric measurements (air temperature, skin temperature, u- and v-components of the wind, atmospheric pressure, relative humidity, and shortwave and longwave radiation), georeference data (latitude, longitude, altitude), and aircraft specific information (roll, pitch, yaw, aircraft height, and ground speed). The UASs were also mounted with an onboard Canon SX110 IS digital camera that collected images of the sea surface. The

ESSDD
5, 1035–1056, 2012

data (except for digital photographs) were recorded on board the aircraft using data loggers and also telemetered back to the field team in real-time during the flights using Iridium satellite communication (when over the horizon) or 900 MHz radio (when within line of sight).

The data was collected by various data loggers on the UAS with varying sampling rates. As part of the quality control process, the data was rigorously checked for false or spurious data as well as streamlined into cohesive sampling rates. The final dataset is provided to the general public in two different formats at a sampling rate of ten seconds. A description of the UAS and flights, the quality control process, and the publically available dataset is provided below.

2 UAS description and flights

During September 2009, the Aerosonde® UAS were flown on sixteen different flights – eight flying north from the Pegasus ice runway near McMurdo Station to TNB, and eight flights flown near Pegasus (Fig. 1). The eight flights near Pegasus were largely test flights used to ensure proper aircraft instrument operations, while the eight flights to TNB were science flights (Table 1). The following describes the standard flight pattern for the science flights to TNB. During the flights to TNB, the aircraft would follow the Transantarctic coast north to TNB, and telemeter data back to the field team at Pegasus Runway via Iridium satellite (Fig. 2). Once the aircraft had done a complete south to north transect of TNB near the coast, the telemetered meteorological data would be used by the mission scientist to locate the position and altitude of strongest winds across TNB. Based on this, a revised set of waypoints and altitudes would then be uploaded in real time to the Aerosonde's autopilot, and the UAS would then fly parallel to the strongest winds (as determined from the telemetered data stream) across TNB (Fig. 3). Along this flight path the UAS performed soundings of the atmosphere at several locations. Figure 4 shows examples of three specific humidity profiles taken along the flight path measured by a UAS on 23 September. Each of these profiles

ESSDD
5, 1035–1056, 2012
Unmanned aircraft system measurements
S. L. Knuth et al.

consisted of a spiral ascent, a spiral descent, or both. The top altitude of each spiral ascent or descent pattern varied by flight but was chosen to ensure the entire depth of the boundary layer was sampled. The local flights near Pegasus Field had no regular and consistent pattern between flights (Figs. 5 and 6).

The Aerosonde® UAS (Maslanik et al., 2002; Curry et al., 2004; Inoue and Curry, 2004; Inoue et al., 2008) are designed and built in Australia for commercial use, and require a field team of four to fly. Extensive, previous use in the Arctic demonstrated the potential of the Aerosonde system for polar operations (Curry et al., 2004). The UAS used for the TNB missions in 2009 had a wingspan of 3 m, a weight of 15 kg, and a payload capacity of 2–5 kg. The aircraft had a range of over 1000 km, and an endurance of 18 h, and were flown between approximately 150 and 3000 m altitude during the flights. The UAS were not flown at a lower altitude due to concerns about the presence of tall icebergs in the area as well as inaccuracies in the GPS altitude data. The planes were manually pilot controlled at take-off and landing and operated in full autonomous mode during most of the flight, with real-time telemetry to the ground station and pilot in command. The pilots had the ability to take over controls or alter the flight plan at any time.

The instruments on board the UAS include both the instruments internal to the UAS as well as additional meteorological instruments added specifically for the 2009 flights. The internal UAS flight management system, including the autopilot, GPS navigational system, flight sensors, communications, and payload interfaces were Piccolo components developed by Cloud Cap Technologies, Inc. Data from the Piccolo system were available on all flights, and were telemetered back in real time. The meteorological instruments added to all of the UAS included pressure data (Vaisala PtB110), skin temperature (Everest Interscience, Inc. Everest 3800ZL), air temperature and relative humidity (Vaisala HMM213), and a nadir-viewing digital camera (Canon Powershot SX110 IS). The u- and v-components of the wind were calculated during aircraft maneuvers. One UAS was also outfitted with Kipp and Zonen CNR2 radiometers to measure shortwave and longwave radiation. An additional GPS, a Canmore GT-730F,

ESSDD
5, 1035–1056, 2012
Unmanned aircraft system measurements
S. L. Knuth et al.

was also added to several UAS. Finally, a laser altimeter was used to measure sea ice freeboard and wave state. This laser altimeter, part of the CU LIDAR Profiling and Imaging System (CULPIS), was designed by the University of Colorado (Crocker et al., 2012). The CULPIS profilometer was designed specifically to collect fine-resolution surface elevation measurements from small UAS in polar environments (Crocker et al., 2012). The system consists of a single-beam near infrared LiDAR sensor that measures the distance from the aircraft to the ground surface at 400 Hz, a L1 GPS unit that detects the aircraft's altitude and location at 10 Hz, and an inertial measurement unit (IMU) that determines the aircraft's attitude and the LiDAR pointing angle at 100 Hz. Due to payload capacity, however, the altimeter was only present on two flights.

3 Data description

There were five data streams in which the data were collected from the UAS – four logger data streams, and one telemetered (Table 2). The telemetered data stream was sent back to the field team in real-time to monitor the aircraft and the weather in which it was flying. The data sent back in real-time consisted of latitude, longitude, altitude, ground speed and direction, roll, pitch, and yaw data, air pressure, air temperature, relative humidity, u- and v-components of the wind, skin temperature, longwave and shortwave radiation, and other data relevant to monitor the aircraft (such as box temperature or instrument voltages). The latitude, longitude, altitude, ground speed and direction, roll, pitch, yaw, air pressure, and u- and v-components of the wind were sourced from the Piccolo avionics. The remaining data was typically the same as that logged onboard the aircraft, but telemetered at a different sampling rate (generally lower) than was logged. The one exception is the u- and v-components of the wind, which were only telemetered and not logged on the on-board data logger.

The final four data streams were from various logger systems on the UAS, with the first of these from the Canmore GPS. The data within this stream consisted of latitude, longitude, altitude, and ground speed, and was only available on certain flights

ESSDD
5, 1035–1056, 2012

(Table 3). The second data stream was the logged analog-to-digital converter (ADC) data that consisted of longwave and shortwave radiation, static air pressure, and skin temperature. The third logged data stream was from the RS232 logger interface consisting of temperature and relative humidity data. The final data stream consisted of the laser altimeter data from the CULPIS instrument. Surface elevation measurements were derived from the LiDAR range data, the GPS position data, and the IMU pointing data during post-processing, although the data from the 2009 TNB flights have not undergone full post-processing.

The data logged onboard and telemetered to the field team were collected at varying sampling rates. The telemetered data was sent back at a sampling rate of 1 Hz when within line of site using the 900 MHz radio link, and at 0.33 Hz when using Iridium connectivity. The logged data from the RS232 was collected at a rate of 0.10 Hz, while the ADC logged data was collected at 10 Hz. The GPS data was logged at a rate of 1 Hz. When the data in the logger file is at a lower sampling rate than the rate at which the telemetered data is provided, the data in the telemetered file is repeated. When the data in the logger file is at a higher sampling rate than the telemetered data, not all of the logger data is included in the telemetered file.

Data was logged and telemetered during pre-flight operations as well as the actual flight of the aircraft. Using the ground speed and altitude data to determine when the UAS was airborne, the five data streams were concatenated to only include data during the actual flight time.

4 Quality control

Quality control (QC) was performed on the data in four of the five data streams as well as synced for similar sampling rates. Spurious data points, unit changes, and other corrections needed to be made in each data set. The CULPIS data provided is the raw LIDAR, GPS, and IMU measurements, and post-processing has not been performed on this data. A summary of the QC process for all other data is provided below.

ESSDD
5, 1035–1056, 2012
Unmanned aircraft system measurements
S. L. Knuth et al.

4.1 RS232 data (temperature and relative humidity)

The data within the RS232 data stream was not time stamped when logged, and extra processing needed to be undertaken to ensure proper accuracy when adding time markers to the data. To accomplish this, the RS232 logged data was compared to the telemetered temperature and relative humidity to determine a matching point between the two files. Because the RS232 logger had a step counter, once an initial matching point was determined, subsequent time markers could be added. This application of time markers could yield an inaccuracy of up to 1–2 s. This is because the telemetered data is occasionally repeated, and when searching for the initial time marker, it can be difficult to determine which value in the telemetered file is the true initial start time.

4.2 ADC data (air pressure, longwave and shortwave radiation, and skin temperature)

The data within the ADC logger file was also not time stamped, but also did have a step counter. However, there were no common data values between the telemetered and ADC logger data to set an initial time stamp, as was true with the RS232 data. In order to set an appropriate time stamp to the ADC logged data, a manual record of when the ADC logger was switched on was used to time stamp the initial value reported in the ADC logged data stream.

The unavailability of comparable data within the two data streams existed for several reasons. First, when the skin temperature and longwave and shortwave radiation voltages from their respective instruments were reported through the telemetered and logger process, the data was compared to two different reference values and calibrated, and thus the final reported value was slightly different for each. Secondly, there were two types of pressure data – the air pressure provided by the Piccolo avionics package, and the air pressure provided from the Vaisala meteorological sensor. Both values were telemetered, but the Vaisala pressure that was telemetered needed to undergo a conversion process, and thus a direct comparison between the two could not be made.

ESSDD
5, 1035–1056, 2012

The Everest skin temperature was also calibrated and corrected via post processing steps due to issues discovered during flight operations. It was determined that when the infrared probe was in a cold environment and sensing a relatively warmer environment (such as when flying above open ocean) the thermometer would report an incorrect value (i.e., instrument housing temperature affected the estimated radiometric temperature). This problem was identified through ground calibration tests done on site. The post-processing corrections were carried out by determining the sensor readings that corresponded to a known low temperature target and a high temperature target. The high temperature target was represented by open water areas during flight, as determined using the Canon aerial photographs. These were assumed to be at a sea-water freezing point of −1.8 °C. Low temperature tie-points were determined by comparing the Everest readings to cold land ice, with temperatures given by near-coincident MODIS satellite data. A linear fit between voltages associated with the low and high temperature targets was then used to convert all voltages to temperatures. This process was done for each flight individually. The estimated error associated with this ad-hoc calibration is about 2 degrees.

4.3 GPS data (latitude, longitude, altitude, ground speed)

The Canmore GPS altitude data was reported as height above the WGS84 ellipsoid rather than altitude above the surface. Consequently, the ellipsoid height needed to be converted to topographic altitude by correcting with the EGM96 datum geoid height, which was found at each latitude and longitude location along the flight path. This correction does not provide the exact height above the surface due to the variable influence of ocean dynamic topography, tides, and atmospheric pressure loading, but it does provide the aircraft mean sea level (MSL) altitude.

ESSDD
5, 1035–1056, 2012
Unmanned aircraft system measurements
S. L. Knuth et al.

4.4 Telemetered data

Very little processing was required of the telemetered data. The altitude reported as part of the Piccolo system was also the ellipsoid height, and also needed to be corrected by the geoid height to obtain the true altitude above the surface. As well, the u- and v-components of the wind provided from the Piccolo were converted into wind speed and direction. The telemetered data was repeated at times such that several different time stamps might have the same data over some time span. In these cases, the first repeated data and time stamp was kept.

Additionally, there are a few instances where one time stamp might report two different values of data – for example, a single time stamp might have two different temperature values. This seemingly repeating time data is actually not repeating data at all, but rather an issue that occurred when the data was telemetered back in real time. Sometimes there would be delays in the transmission of telemetered data that would cause several data packets to be sent at once. Typically when there is repeating data there is a data gap that occurs adjacent to the data. However, because the correct time of the repeated data cannot be accurately determined, the data in the file has been left as is.

5 Data availability

The data from the September 2009 flights has been submitted to the United States Antarctic Program Data Coordination Center (USAP-DCC) (doi:10.1594/USAP/0739464). The available data is in text and csv formats, and is provided at ten-second intervals, representing the lowest sampling rate of the logged data, with an accuracy to within five seconds (Table 4). The data from the flights provided in these files are: date and time, latitude, longitude, altitude, temperature, relative humidity, pressure, wind speed, wind direction, the u- and v-components

Discussion Paper | Discussion Paper | Discussion Paper | Discussion Paper |

ESSDD

5, 1035–1056, 2012

Unmanned aircraft system measurements

S. L. Knuth et al.

of the wind, longwave and shortwave radiation, skin temperature, ground speed and direction, roll, pitch, and yaw, and laser altimeter.

As described in Sect. 3, there are several instruments that might provide duplicate data (for example, on flights when the Piccolo and Canmore GPS are used). As such, there is a hierarchy to the type of data that is provided in the final dataset. Typically, data provided by instruments that are not part of the Piccolo system, and were added specifically as part of the 2009 flights, are used whenever available. This impacts latitude, longitude, altitude, pressure, and ground speed data. If the Canmore GPS data is available, the latitude, longitude, and altitude from that device will be used over the Piccolo GPS data. The only exception to this is the ground speed data. Because the Canmore GPS did not provide ground direction data, the ground speed and direction data reported is always from the Piccolo system.

Because the Piccolo air pressure was not used during flight operations and therefore was not properly calibrated, the Vaisala air pressure was used whenever available. In instances where the Piccolo air pressure needed to be used, the data was rigorously analyzed to ensure validity. The air pressure at flight take-off and landing was compared to a local automatic weather station at the Pegasus ice runway to determine both accuracy and that any differences between the two pressures at take-off were the same when the aircraft landed. For all flights where the Piccolo air pressure was used, it was deemed to be accurate.

6 Summary

In September 2009, a series of long-range unmanned aircraft system flights were made to Terra Nova Bay, Antarctica to study changes in the atmospheric boundary layer overlying a latent heat polynya during winter conditions. Eight flights were flown on science missions to Terra Nova Bay, with an additional eight flights flown near the Pegasus ice runway (the origin of the UAS flights) as test flights to ensure proper aircraft operations. The data was quality controlled and processed, and has been submitted to

ESSDD
5, 1035–1056, 2012

the USAP-DCC data repository for public use. The data available at the USAP-DCC consists of date and time, latitude, longitude, altitude, temperature, relative humidity, pressure, wind speed, wind direction, the u- and v-components of the wind, longwave and shortwave radiation, skin temperature, ground speed and direction, and roll, pitch, and yaw provided at ten second intervals for all sixteen flights. The laser altimeter data for two of the flights is also provided.

Acknowledgements. The authors wish to thank Michael Willis of Cornell University and Seth White of UNAVCO for their assistance with the technical aspects of understanding geoid and ellipsoid heights. This work is supported by NSF grant ANT 0739464.

References

Cassano, J. J., Maslanik, J. A., Zappa, C. J., Gordon, A. L., Cullather, R. I., and Knuth, S. L.: Observations of Antarctic Polynya With Unmanned Aircraft Systems, EOS, 91, 245–246, doi:10.1029/2010EO280001, 2010.

Ciappa, A., Pietranera, L., and Budillon, G.: Observations of the Terra Nova Bay (Antarctica) polynya by MODIS ice surface temperature imagery from 2005 to 2010, Remote Sens. Environ., 119, 158–172, 2012.

Crocker, R. I., Maslanik, J. A., Adler, J. J., Palo, S. E., Herzfeld, U. C., and Emery, W. J.: A sensor package for ice surface observations using small unmanned aircraft systems, IEEE T. Geosci. Remote Sens., 50, 1033–1047, 2012.

Curry, J. A., Maslanik, J. A., Holland, G., Pinto, J., Tyrrell, G., Inoue, J.: Applications of Aerosondes in the Arctic, B. Am. Met. Soc., 85, 1855–1861, 2004.

Inoue, J. and Curry, J. A.: Application of Aerosondes to high-resolution observations of sea surface temperature over Barrow Canyon, Geophys. Res. Lett., 31, L14312, doi:10.1029/2004GL020336, 2004.

Inoue, J., Curry, J. A., and Maslanik, J. A.: Application of Aerosondes to melt-pond observations over Arctic sea ice, J. Atmos. Ocean. Tech., 25, 327–334, 2008.

Kurtz, D. D. and Bromwich, D. H.: Satellite observed behavior of the Terra Nova Bay polynya, J. Geophys. Res., 88, 9717–9722, 1993.

Maslanik, J. A., Curry, J., Drobot, S., and Holland, G.: Observations of sea ice using a low-cost unpiloted aerial vehicle, Proc. 16th. IAHR International Symposium on Sea Ice, Int. Assoc. of Hydraulic Engineering and Research, 3, 283–287, 2002.

ESSDD

5, 1035–1056, 2012

Unmanned aircraft system measurements

S. L. Knuth et al.

Table 1. Start and end times (in UTC) and the UAS aircraft number for science flights to TNB and local flights near Pegasus ice runway.

Science Flights		Local Flights	
Start – End Times	UAS Number	Start – End Times	UAS Number
Start: 14 Sep 04:37:28 End: 14 Sep 19:39:45	214	Start: 7 Sep 00:14:38 End: 7 Sep 01:04:08	217
Start: 18 Sep 03:02:54 End: 18 Sep 19:39:00	214	Start: 8 Sep 21:02:20 End: 9 Sep 03:47:30	217
Start: 21 Sep 18:51:54 End: 22 Sep 05:51:32	214	Start: 9 Sep 00:56:57 End: 9 Sep 05:29:31	214
Start: 23 Sep 19:09:10 End: 24 Sep 06:24:48	215	Start: 10 Sep 05:58:57 End: 10 Sep 06:26:07	214
Start: 23 Sep 20:08:09 End: 24 Sep 06:13:28	216	Start: 12 Sep 04:02:24 End: 12 Sep 04:52:24	215
Start: 25 Sep 06:50:11 End: 25 Sep 19:41:38	215	Start: 13 Sep 04:38:49 End: 13 Sep 21:44:35	214
Start: 26 Sep 18:33:46 End: 27 Sep 04:35:04	214	Start: 16 Sep 03:20:19 End: 16 Sep 06:30:39	215
Start: 26 Sep 19:23:40 End: 27 Sep 04:19:51	216	Start: 22 Sep 04:52:04 End: 22 Sep 06:18:34	216

ESSDD
5, 1035–1056, 2012

Table 2. Data available in the four logger and one telemetered data streams. Sampling rates are also given.

Telemetered (0.33–1 Hz)	Latitude Longitude Altitude Ground Speed Ground Direction Roll Pitch Yaw	Air Temperature Air Pressure Relative Humidity Longwave Radiation Shortwave Radiation Skin Temperature u-Component of Wind v-Component of Wind
GPS (1 Hz)	Latitude Longitude	Altitude Ground Speed
ADC (10 Hz)	Longwave Radiation Shortwave Radiation	Air Pressure Skin Temperature
RS232 (0.10 Hz)	Air Temperature	Relative Humidity
CULPIS	Laser Altimeter	

ESSDD
5, 1035–1056, 2012
Unmanned aircraft system measurements
S. L. Knuth et al.

Table 3. Available data for each of the sixteen September 2009 flights.

	RS232	GPS	ADC	Telemetered
7 Sep, #217				X
8 Sep, #217				X
9 Sep, #214				X
10 Sep, #214				X
12 Sep, #215				X
13 Sep, #214	X			X
14 Sep, #214	X	X		X
16 Sep, #215				X
18 Sep, #214	X	X		X
21 Sep, #214	X		X	X
22 Sep, #216	X	X	X	X
23 Sep, #215	X		X	X
23 Sep, #216	X	X	X	X
25 Sep, #215	X		X	X
26 Sep, #214	X	X	X	X
26 Sep, #216		X	X	X

ESSDD
5, 1035–1056, 2012
Unmanned aircraft system measurements
S. L. Knuth et al.

Table 4. A sample of the data available in the USAP-DCC repository.

Day	Hour	Minute	Second	Lat (deg)	Lon (deg)	Altitude (m)	Temp (C)	RH (%)	Pressure (Pa)	Wind Speed ($m s^{-1}$)	Wind Direction (deg)
23	20	8	9.54	-77.95	166.49	4.71	-33.89	70.67	100378.09	0	0
23	20	8	19.54	-77.95	166.49	5.70	-35.61	70.41	100354.58	0	0
23	20	8	29.54	-77.95	166.49	3.54	-36.31	70.67	100255.65	7.61	231.50
23	20	8	39.54	-77.95	166.49	33.88	-30.6	73.05	99866.85	1.93	236.14

ESSDD
5, 1035–1056, 2012

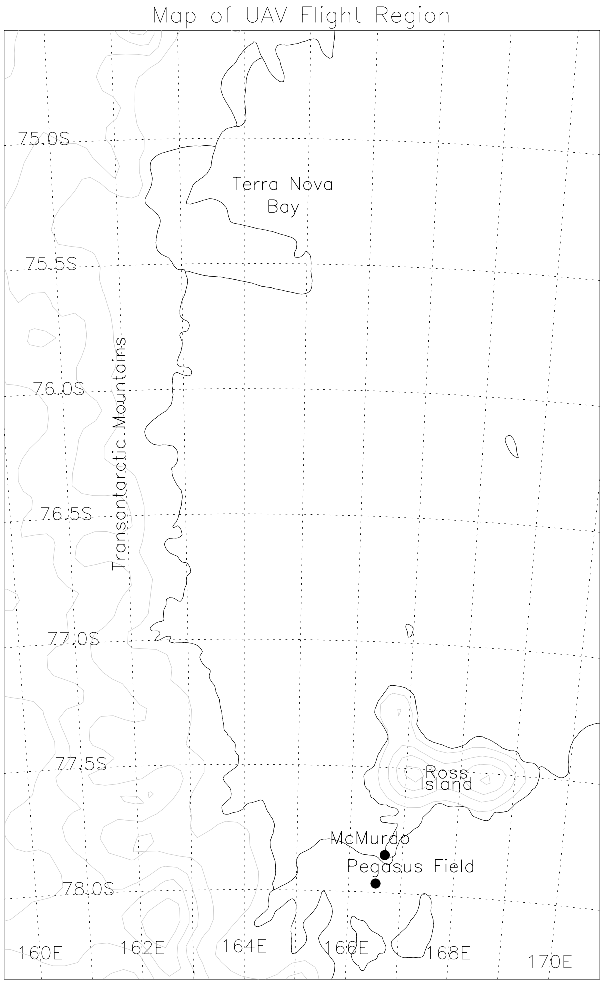

Fig. 1. Map of the entire UAS flight region, from Pegasus Runway to Terra Nova Bay.

ESSDD

5, 1035–1056, 2012

Unmanned aircraft system measurements

S. L. Knuth et al.

Title Page

Abstract | Instruments

Data Provenance & Structure

Tables | Figures

◀| |▶

◀ ▶

Back | Close

Full Screen / Esc

Printer-friendly Version

Interactive Discussion

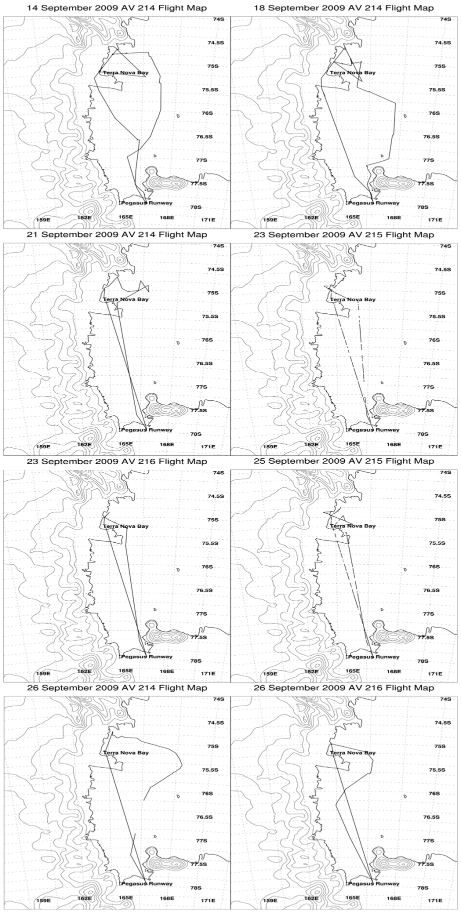

Fig. 2. Eight flights from Pegasus Runway to Terra Nova Bay. Gaps in the flight path indicate a lack of data.

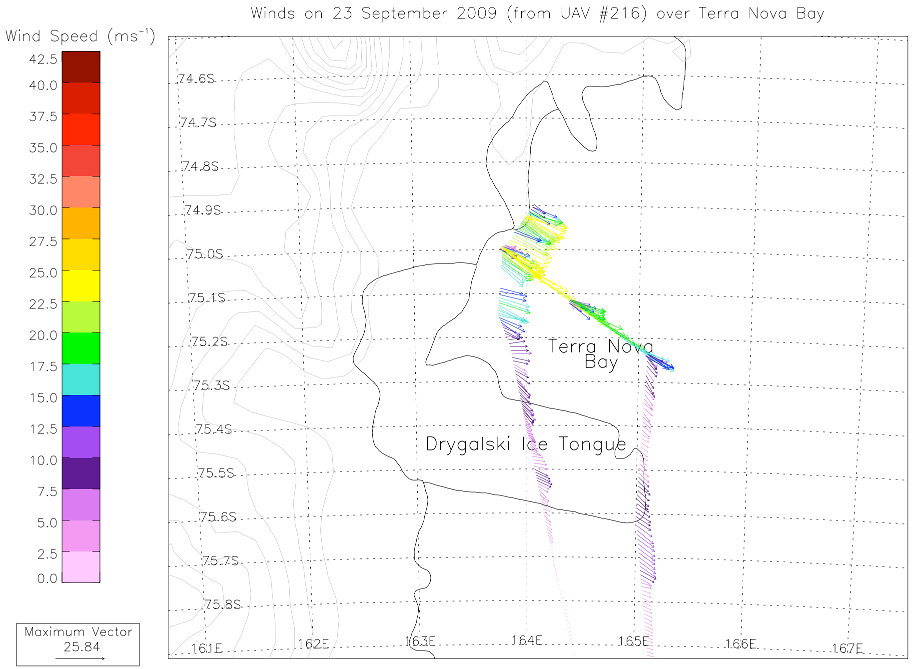

Fig. 3. Winds on 23 September 2009 UAS flight over Terra Nova Bay.

ESSDD
5, 1035–1056, 2012

Unmanned aircraft system measurements

S. L. Knuth et al.

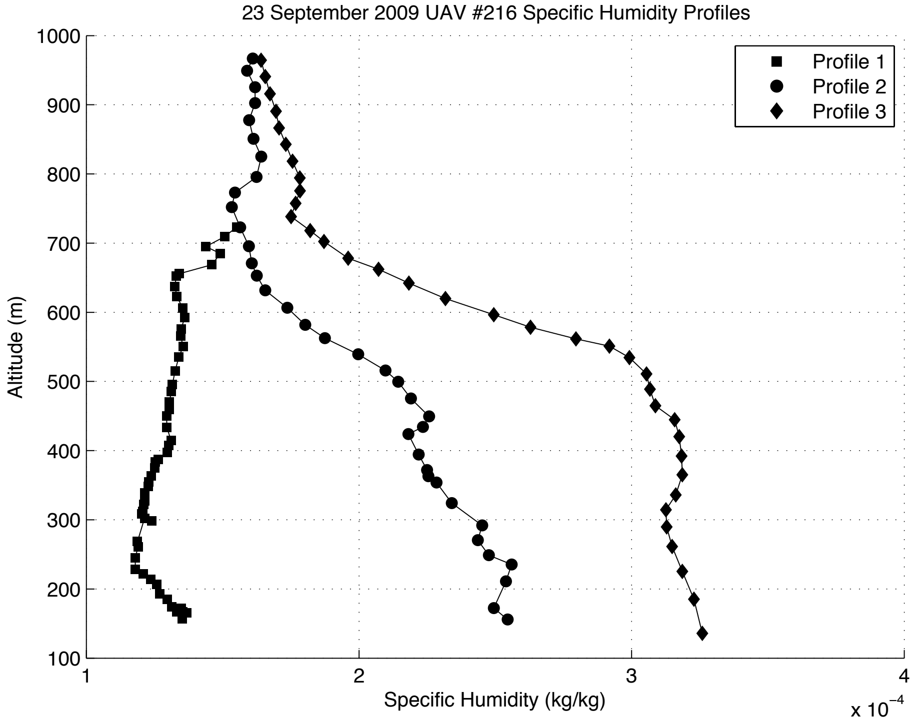

Fig. 4. Specific humidity profiles from the 23 September 2009 (UAS #216) flight.

ESSDD

5, 1035–1056, 2012

Unmanned aircraft system measurements

S. L. Knuth et al.

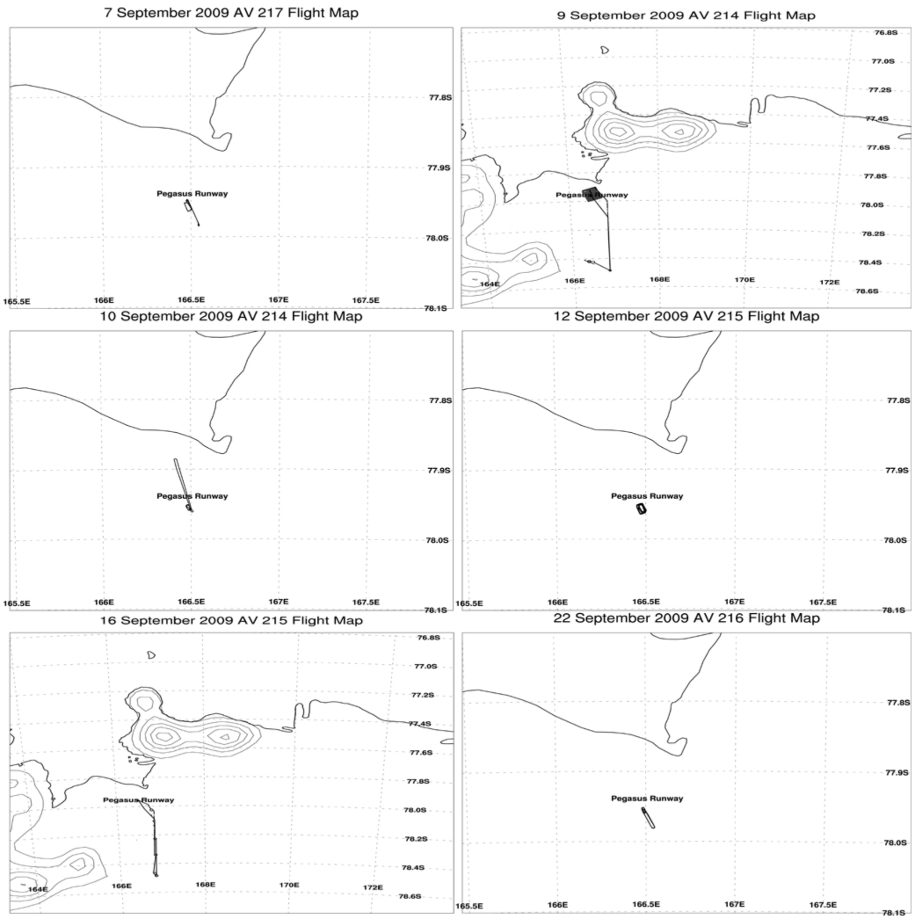

Fig. 5. Six of the local flights near Pegasus Runway. Gaps in the flight path indicate a lack of data.

ESSDD
5, 1035–1056, 2012

Title Page
Abstract | Instruments
Data Provenance & Structure
Tables | Figures
Back | Close
Full Screen / Esc
Printer-friendly Version
Interactive Discussion

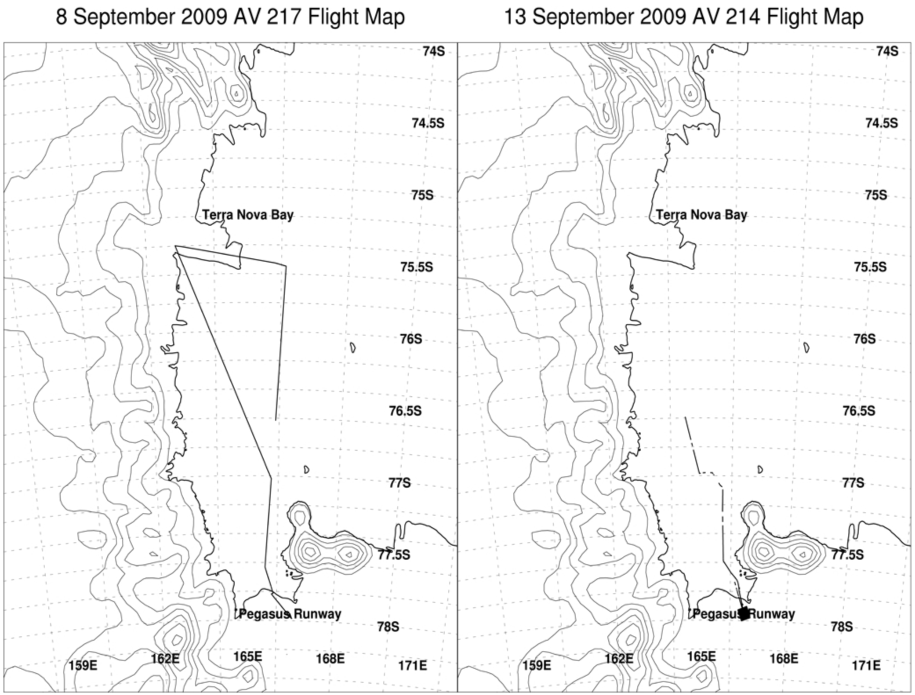

Fig. 6. Two remaining local flights that did not reach Terra Nova Bay. Gaps in the flight path indicate a lack of data.

ESSDD
5, 1035–1056, 2012

Unmanned aircraft system measurements

S. L. Knuth et al.